Spring 5-2013

# Exploring the Interactions Between Interleukin-8 (IL8) and Amyloid-**β** (A**β**) Peptide in Traumatic Brain Injury

Olivia G. Gibson
*University of Southern Mississippi*

Exploring the interactions between interleukin-8 (IL8) and amyloid-β (Aβ) peptide in traumatic brain injury

By

Olivia Gibson

A Thesis
Submitted to the Honors College of
The University of Southern Mississippi
In Partial Fulfillment
Of the Requirements for the Degree of
Bachelor of Science
In the Department of Chemistry and Biochemistry

April 2013

Approved By

_____

Vijay Rangachari, Ph. D.

Department of Chemistry and Biochemistry

_____

Sabine Heinhorst, Ph. D.

Department of Chemistry and Biochemistry, Chair

_____

David R. Davies, Ph. D.

Honors College, Dean

# Abstract

Alzheimer's disease (AD) is a neurodegenerative disorder characterized by cognitive dysfunction and memory loss, and pathologically characterized by amyloid-beta (Aβ) plaques and inflammation. Recent research has shown that these Aβ plaques are also found in traumatic brain injury (TBI) patients. This discovery has led to a proposed pathway leading from traumatic brain injuries to dementia, more specifically AD. After a TBI, human granulin-A (GRN) and interleukin-8 (IL8) are released and the number of elastases in the brain increases in response to the inflammation response. IL8 is a cytokine that is released in acute inflammation responses, and the levels of IL8 secreted are increased. Because of the presence of Aβ plaques in the brains of TBI patients soon after the initial injury, it can be hypothesized that IL8 plays a role in the aggregation of these Aβ plaques because of the inflammation response associated with this cytokine, as well as the increased presence of IL8 in the brain. In order to examine the possible interactions between IL8 and Aβ, the protein IL8 is being recombinantly expressed in E. coli, and then purified using a nickel column. After purification, the protein will be characterized using circular dichroism (CD), Ellman's Assay, and mass spectrometry. The interactions between IL8 and Aβ are being examine using ThioflavinT (ThT) fluorescence and SDS-PAGE. When the results of the purification are examined, they show that the protein obtained was pure and in the correct conformation. The interaction studies using ThT showed inhibition of Aβ aggregation in the presence of IL8. Overall, the results from the research indicate that IL8 does play an inhibitory role in the aggregation of Aβ.

# **<u>Table of Contents</u>**

# Introduction

Alzheimer's disease (AD) is a progressive, neurodegenerative disorder that is characterized by cognitive dysfunction and memory loss, and is the most common form of dementia. Pathologically, this disease is characterized by the presence of amyloid-β (Aβ) plaques, neurofibrillary tangles, and neuronal death and loss of synapse functioning (*1*). Memory loss and cognitive dysfunction, as well as the other symptoms of AD, are caused by the deposition of the Aβ plaques in the brain that result in the death of neurons and the atrophy of brain tissue. The plaques that are present in the brains of AD patients are dense-core plaques, often referred to as "senile" plaques. These plaques are located around the neurons and result in neuronal death; the death of the neurons causes the loss of synaptic functioning and information is no longer able to be transmitted via these synapses. Each Aβ plaque is composed of an accumulation of amyloid-β fibers formed from the Aβ peptide, which is synthesized in the neuronal membrane in cholesterol-rich regions and then released into the extracellular space (*3*). Aβ peptides are generated by the proteolytic processing of amyloid precursor protein (APP) (*9*). Aβ peptides typically range from 37 to 43 amino acids among which Aβ40 peptide, and the Aβ42, are the common ones (*1,13*). Because the Aβ42 aggregates at a faster rate, it is commonly observed in the prefibrillar aggregates and dense-core plaques (*1*). The process of Aβ peptide aggregation nucleation-dependent in which a conformationally-altered aggregate forms a nucleus for further aggregation. Typically, monomeric Aβ aggregates to forms a nucleus which then seeds the formation of protofibrils and fibrils as shown in in Figure 1.
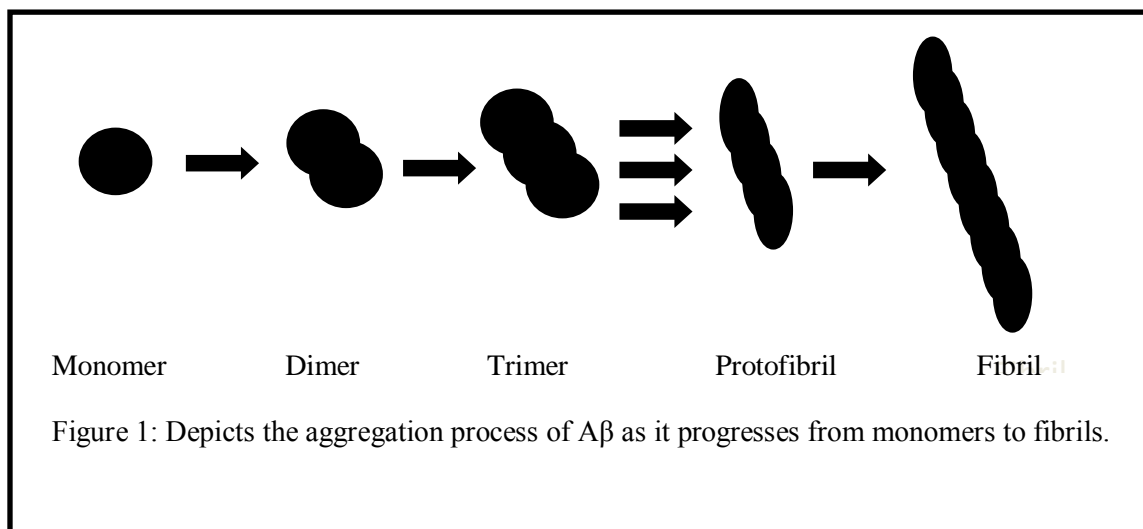
Figure 1: Depicts the aggregation process of Aβ as it progresses from monomers to fibrils.

While Aβ plaques are believed to be one of the toxic species, another problematic pathological characteristic of AD is the presence of these neurofibrillary tangles. Neurofibrillary tangles cause damage to the neurons in the brains of Alzheimer's disease patients, and these tangles are found in and around the neurons and are large bundles of abnormal fibers that lack membrane-binding; the individual fibers are found in pairs in helical structures (*1*).    The major component of the neurofibrillary tangle is tau, a soluble protein located in the cytoplasm (*1, 2*).  Tau is a structural component of microtubules, and mutated tau is found in the tangles.  The formation of these plaques results in neuronal damage, and this ultimately causes the neurons to die; when combined with Aβ plaque deposition, neuronal death and damage leads to inflammatory responses *(2,4)*.

Inflammatory responses have been shown to play a role in Alzheimer's disease. The innate branch of the immune system is responsible for clearing the Aβ deposits, but the plaques that the immune system can't clear are responsible for the chronic inflammation in AD (*5,11,14*).  The complement pathway activated is the alternative

pathway, but the classical complement pathway has also been found to operate in AD (*11, 19*). The end result of both pathways, the formation of the membrane-attack complex (MAC), is the same (*19*). The MAC "punches" holes in the membrane of the targeted molecule, and the accumulation of these holes results in the death of the targeted molecule; however, the death of the cell causes the contents to be released into the environment and an inflammation response to occur. In healthy brains, formation of MAC is a positive response because the foreign cell will lyse when enough MACs are present; however, neuronal membranes with MACs that are located near Aβ plaques results in damage to healthy cells (*11*). Alternative complement pathways do not need antigen and antibody to bind in order to initiate the pathway, so it is usually activated by foreign molecules on cell surfaces (*19*). Unlike the alternative pathway, the classical complement pathway is an adaptive form of immunity. To activate classical complement, antigen and antibody must bind (*19*). In the case of AD, the Aβ plaques cause the alternative complement system to be activated because the senile plaques are labeled foreign by the immune system. While the alternative complement pathway is activated, the plaques are unable to be cleared, resulting in a chronic inflammatory response. Aβ plaques, however, are not the only triggers for chronic inflammation in the AD pathway. Accumulation of the neurofibrillary tangles also results in inflammation in the brain of Alzheimer's patients, and this typically occurs after failed attempts by the innate immune system to remove the dead neurons (*20*). The combination of the senile plaques and neurofibrillary tangles results in an overall inflammatory response in the brain, causing an increase in neuronal death.

Alzheimer's disease is not the only neurodegenerative condition that involves an inflammatory response. The Centers for Disease Control and Prevention describes a TBI as an event that causes a penetration or contusion with the head that impairs normal brain functioning (*22*). Traumatic brain injuries are also classified as neurodegenerative disorders because of the damage that occurs to the brain tissue that causes degenerating neural conditions (*23*). These injuries also exhibit inflammatory responses similar to those seen in the AD pathway; TBI injuries are believed to initiate dementia, but the molecular mechanism is unknown. The proposed pathway of TBI leading to dementia is given in Figure 2.



Figure 2: Proposed pathway of TBI leading to dementia.
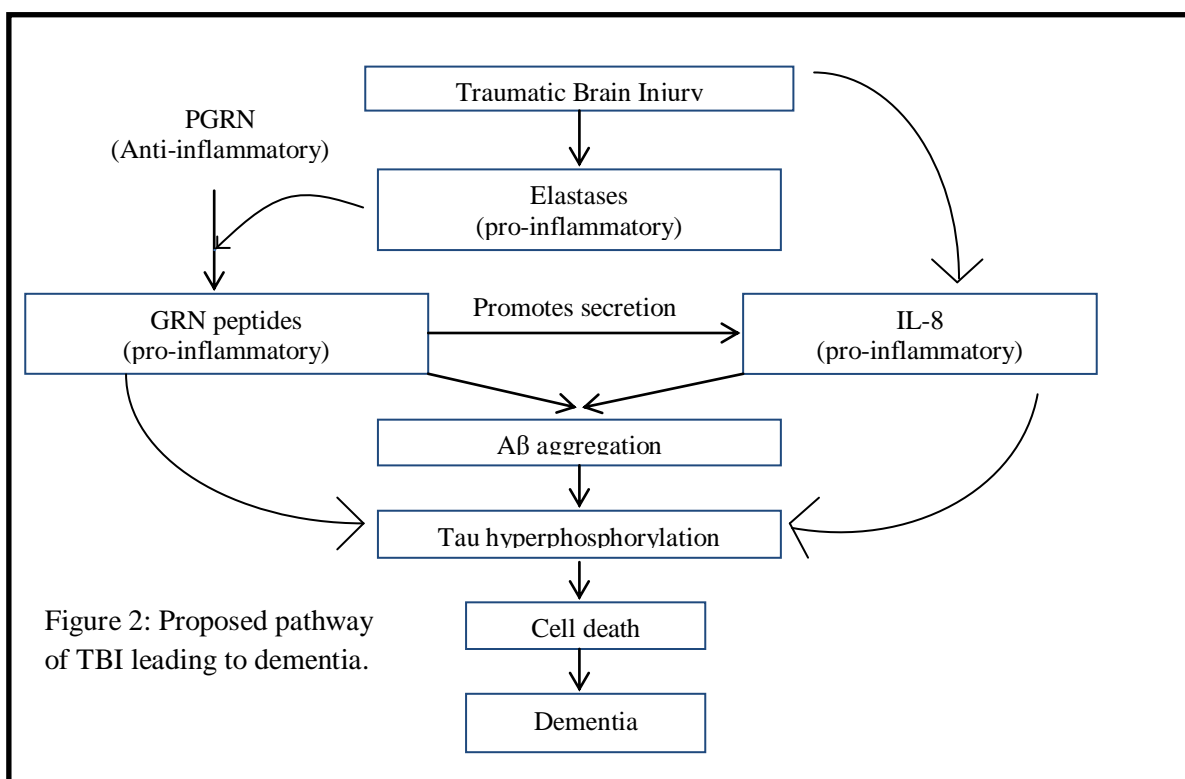
Immediately after a traumatic brain injury, interleukin-8 (IL8), one of the cytokines is released along with a number of elastases. Progranulin (PGrn), an anti-inflammatory protein is then cleaved by the elastases into smaller granulin (Grn) peptides (*4*). When an

injury occurs, progranulin is upregulated and secreted (*3,7*).In a recent study, it was found that progranulin is useful for wound repair and granulation, knowledge that could be applied to treatment of inflammation (*8*).   Granulins in turn may promote the secretion of IL8, and granulin has recently been shown to be involved in Aβ aggregation (*7*).  Both IL8 and Grns are pro-inflammatory that are likely mediators in acute inflammation-triggered Aβ aggregation.  In this study we are focused on IL8 and its interaction with Aβ.  PGrn is 593 amino acid residues rich in cysteine.  Granulin peptides are growth factors like their precursor, progranulin, that are involved in wound repair, tumor growth, and inflammation (*4*). Grn contains 12 cysteines and is approximately 6 kDa in size (*16*).  Recently, it was discovered that granulin peptides promote the secretion of IL8 (*7*).  Since Grn peptides and IL8 are both pro-inflammatory, and AD involves an inflammation response, it is thought that they could each play a role in the aggregation of the Aβ plaques because of the presence of these dense-core plaques within hours of traumatic brain injury.   There is limited information about the IL8 involvement in AD; because the peptides that secrete IL8 have been linked to AD, there may be an interaction between IL8 and the Aβ.

IL8 is the pro-inflammatory pathway component of interest in this study, and it is involved at two different stages and is believed to be involved in Aβ aggregation.  IL8 is a member of the chemokine alpha family, indicating that the genes for IL8 are found on chromosome 4 (*15*).  A chemokine is a chemotactic cytokine with a low molecular weight and functions as an inflammation factor (*12*).  Chemokines trigger inflammation in a specific manner because they have a highly basic nature, causing them to attract inflammatory cells that are in the bloodstream by interacting with the acidic extracellular

components found in the matrix (*15*). The structure of the IL8 chemokine is a C-X-C

organization, which is two cysteines with an amino acid located between them, and the

entire structure consists of 72 amino acids (*3, 15*). The secondary structure of IL8

consists of two alpha helices and six beta sheets.

Because of the pro-inflammatory characteristics of IL8 and it upregulation in

traumatic brain injury, it is hypothesized that this protein plays a role in the aggregation

of Aβ in Alzheimer's disease, and these potential interactions were examined using

various biochemical and biophysical methods, such as thioflavin-T (ThT) fluorescence

and SDS-PAGE.

# Materials and Methods

*Materials*

The pET-15b expression vector containing the gene of IL8 protein was synthesized at Florida State University, and the Aβ42 peptide was synthesized by the Mayo Clinic peptide synthesis facility.  SDS and ThT were purchased from Sigma Aldrich, and the other compounds and chemicals use d were purchased from VWR, inc.

*Methods*

*Interleukin-8 Expression*

The protein was expressed by inoculating the BL21 *E. coli* with the plasmid.  The protein consisted of a His-tag and a thrombin cleavage site (Figure 3).



Figure 3: Construct that was inserted into the vector with His-tag, IL8, and cleavage
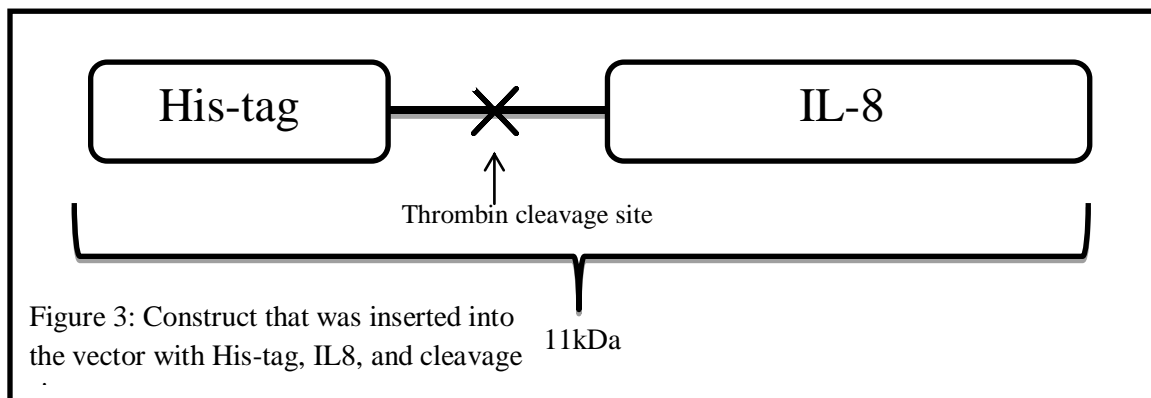
To start the cultures, 5 mL of Luria Bertani (LB) broth was added to a 15 mL culture tube, then ampicillin was added in the concentration of 1 mg/mL.  A cotton swab was then used to obtain small quantities of frozen IL8 from the 2-5 colony in the $-80^0$C, and the cotton swab was placed in the culture tube overnight and left to shake in the $37^0$C incubator.  Next, 3 mL of the overnight culture was added to a 1 L culture of LB broth with ampicillin and allowed to shake in the $37^0$C incubator until the optical density

reached 0.6-0.8, and when this $OD_{600}$ level is reached, the culture was induced using 0.5 mM isopropylthio-β-galactoside (IPTG) and then returned to the incubator for three more hours. The cells were then placed in a 50 mL conical tube and centrifuged for 10minutes at 9500 rpm using a Beckman Coulter Allegra X-22R centrifuge; the supernatant was discarded and the pellet was kept for purification.

*Protein Purification*

After the cells had been expressed, the pellet is resuspended in 15 mL of 8 M Urea, and 1 mM phenylmethanesulfonyl fluoride (PMSF), a serine protease inhibitor, was added. The pellet was then vortexed to thoroughly resuspend the protein. Once the protein was back in solution, the resuspended pellet was sonicated to break open the cells and release the protein from the inclusion bodies. The sonication was performed using a Misonix Ultrasonic Liquid Porcessor XL-2000 probe sonicator on ice for 30 seconds on and 30 seconds off for a total of four cycles, and then the sonicated pellet shook for a minimum of five hours on the orbital shaker. After at least five hours, the cell lysate was centrifuged at 9500 rpm for 10 minutes in order to the remove the cell debris. The cell debris formed the pellet and the resulting supernatant was saved because this is the fraction that contained the protein.

Before the protein could be purified using the nickel column, the column had to be equilibrated using 30 mL of Loading Buffer that contained 20 mM Tris pH 7.0, 100 mM NaCl, 10 mM Imidazole, and 2 M Urea. The supernatant was then loaded onto the column, and the flowthrough was collected by slowly running the sample through the column. This fraction was collected and stored at $4^0$C. 100 mL of Wash buffer was then

run through the column, and this wash contained 20 mM Tris pH 7.0, 100 mM NaCl, 150 mM Imidazole, and 2 M Urea. The wash fraction was collected and stored at $4^0$C. Following the wash, the protein was eluted by washing the column with 15mL of Elution Buffer, and this consisted of 20 mM Tris pH 7.0, 100 mM NaCl, 400 mM Imidazole, and 2 M Urea. The elution fraction was collected and stored at $4^0$C. The final step of the purification column was to rinse the column using 25 mL of Strip Buffer than contained 20 mM Tris, 250 mM EDTA, and 50 mM NaCl pH 8.0, and this fraction was also collected and stored at $4^0$C.

The elution fraction was then dialyzed to remove the remaining Imidazole that was in the protein sample, and this was done using a 3.5 kDA membrane. The fraction was pipetted into the membrane and the membrane was secured from leaks before being placed in the buffer. For this dialysis, the buffer used contained 20 mM Tris, 150 mM NaCl, and 1 M Urea at pH 9.0, and the dialysis was conducted at $4^0$C. The buffer was changed a minimum of three times before the protein was removed from the membrane and stored in a conical tube at $4^0$C.

In order to ensure the purity of the protein collected, a gel was run using a 12% polyacrylamide gel in 1X TRIS-glycine-SDS buffer, pH 6.8 at 80 V. The flowthrough, wash, elution, dialyzed, and strip fractions were all run in the gel, and the samples included 15 mL of the fraction and 5 mL of sample buffer. After the gel was run, it was stained using GelCode Blue, obtained from Thermo Scientific, and the bands were examined to determine if the protein was pure.

*Purification Protocol Modifications*

Modifications to the purification protocol include shaking the supernatant on the column overnight before collecting the flowthrough, and the concentrations of urea were changed in the different buffers. Instead of using one wash to rinse the column, three washes were used so the concentration of the urea could be gradually decreased. The loading buffer was changed to include 20 mM Tris pH 7.0, 10 mM Imidazole, and 6 M Urea pH 6.5. Wash 1 contained 20 mM Tris pH 7.0, 100 mM Imidazole, and 4 M Urea pH 6.5; wash 2 was composed of 20 mM Tris, 150 mM Imidazole, and 2 M Urea pH 6.5; and wash 3 contained 20 mM Tris pH 7.0 and 150 mM Imidazole.

*Concentration of the Protein*

Once the protein was purified, the concentration of the resulting fraction was determined using Cary UV spectrophotometer. The Cary UV Scan program was used to obtain a baseline and then the concentration of the protein. The baseline sample was 70 μL of the dialysis buffer, and the protein sample was 70 μL of the dialyzed protein. For both samples, the absorbance was set at 280 nm. The graph of the scanned dialyzed protein was used to calculate the concentration. A line was drawn from the flattest part on the right-hand side of the graph to the y-axis and a line was drawn parallel to the y-axis at the 280 nm mark. The length of the line from the peak to where it intersects the bottom line was measured in millimeters, and the distance between two numerical points on the y-axis was measured in millimeters. The length of the line from the peak to the bottom line was divided by the distance between the two points on the y-axis, and this value was multiplied by the value that separated the points on the y-axis; the calculated value was then divided by the known extinction coefficient, 7240.

*Ellman's Assay*

The Ellman's Assay was done following the Thermo Scientific protocol for Quantifying Sulfhydryl Groups Based on Molar Absorptivity.  For this procedure, a reaction buffer containing 0.1 M sodium phosphate pH 8.0 and 1 mM EDTA was made, and an Ellman's reagent solution solution was prepared by dissolving 4 mg Ellman's reagent in 1 mL of the prepared reaction buffer.  A baseline sample containing 5 µL of Ellman's reagent, 250 µL reaction buffer, 20 µL of Tris, and 5 µL of water was prepared and incubated at room temperature for five minutes.  The sample containing the protein was prepared using 5 µL of Ellman's reagent, 250 µL of reaction buffer, 20 µL IL8, and 5 µL of water, and this sample was also incubated at room temperature for five minutes. The spectrophotometer was set to scan from 350 nm to 450 nm, and the instrument was calibrated using the baseline sample before running the protein sample.  After cleaning the cuvette, the protein sample was pipetted into the cuvette and the absorbance was measured.  The graph was printed out and the concentration of cysteines in the sample was calculated by drawing a line parallel to the x-axis following the flattest region of the curve and intersecting as many points along the line as possible.  A line parallel to the y-axis was then drawn at the 412 nm wavelength, and the length of this line to where it intersected the previously drawn line was measured in millimeters.  The distance between two of the absorbance units on the y-axis was then measured in millimeters.  The length of the line at 412 nm was divided by the distance between the two points on the y-axis, and this is multiplied by the difference in numerical value between the points on the y-axis.  After this value was calculated, the value was divided by the extinction coefficient

of 2-nitro-5-thiobenzoic acid (TNB), $14{,}150 \ M^{-1}cm^{-1}$, and the value was converted into micromolar to examine the concentration.

*Circular Dichroism*

Circular Dischroism (CD) was performed using a Jasco J-815 spectropolariometer that was set to monitor continuously from 190 nm to 260 nm, and each sample was run three times and the values averaged. The samples were placed in a 0.1 cm quartz cuvette, and 140 µL of each sample, Aβ control, IL8 control, and Aβ/IL8 interaction, was used to examine the secondary structure.

*Mass Spectrometry*

MALDI-TOF mass spectrometry was performed by spotting a mass spectrometry plate with the IL8 sample. The spectrometer was used to examine the molecular weight of IL8 in order to confirm the purity of the protein.

*Thioflavin-T Fluorescence*

ThT Fluorescence was monitored using a Cary Eclipse fluorescence spectrophotometer that was set to an excitation wavelength of 450 nm, emission wavelength of 482 nm, and slit widths of 10 nm. Samples were made for an Aβ control, IL8 controls, and Aβ/IL8 interaction samples. The Aβ control 25 µM Aβ, 50 mM NaCl, and was filled to 100 µL with Tris pH 7.0. The IL8 controls were done in concentrations of 12.5 µM, 24 µM, and 50 µM, and each contained 50 mM NaCl and were filled to a total volume of 100 µL with Tris pH 7.0. In order to determine the fluorescence of each sample, a 1 cm quartz microcuvette was filled with 70 µL of 10 µM ThT and 5 µL of a

sample. The fluorescence spectrum was calculated and the absorbance at 0.5 A.U. was recorded. The fluorescence was taken for each sample every 24 hours, with the samples being stored at $37^0$C, and the points were plotted on a graph to examine the interactions.
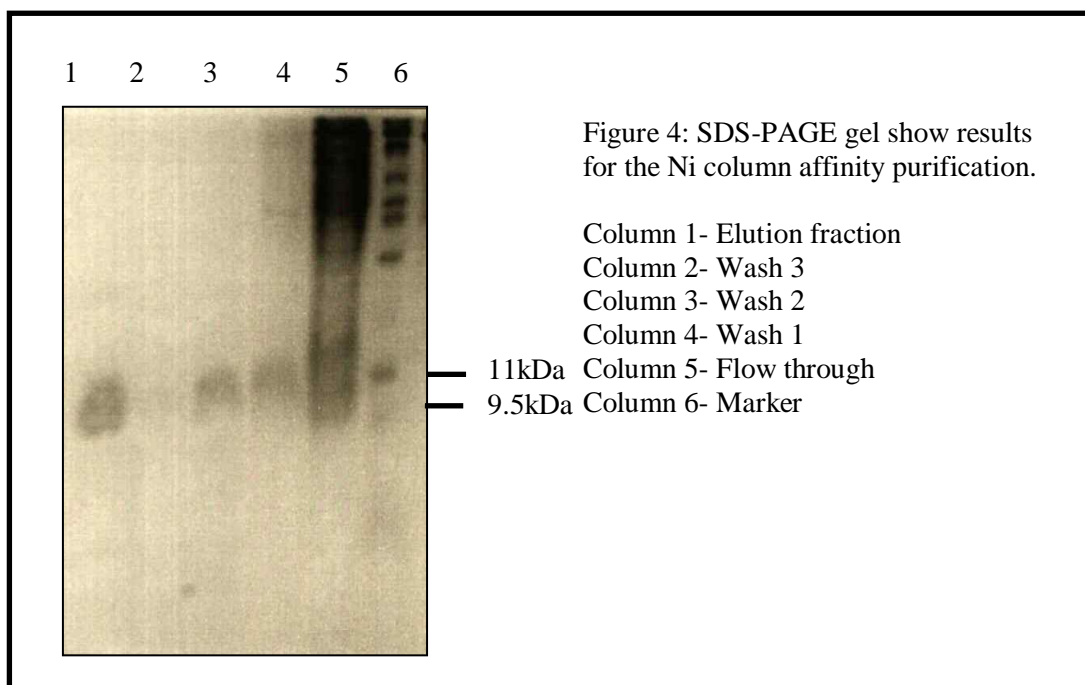
*SDS-Page and Silver Stain*

The gels used in the polyacrylamide gel electrophoresis were handmade 12% polyacrylamide gels, and the gels were run at 80 V in 1X Tris-Glycine-SDS, pH 6.8 buffer. The samples contained 5 µL of 4x sample buffer and 15 µL of the sample being examined. When a silver stain was being used with the gel, an unstained marker was used.

For a silver stain, the staining kit was purchased from Thermo Scientific and the Thermo Scientific protocol was followed in the development of the gel. The gel was washed in nanopure water for two five minutes washes, placed in silver stain fixing solution for fifteen minutes, washed with 10% ethanol solution for two five minute washes, rinsed with nanopure water for two more five minute washes, treated with sensitizing solution for one minute, rinsed with water for two one minute washes, incubated in working stain for thirty minutes, rinsed with water for two twenty second rinses, and then placed in developing solution. The developing solution was left on the gel until the bands were clearly visible, then the developing solution was replaced with silver stain stop solution.

## Results

*Protein Purification*

After the protein was expressed in the *E. coli* cells, the cells were lysed and centrifuged to collect the protein, and the cells were clarified for Ni-affinity purification as described in the Materials and Methods.  The ability to obtain a pure protein was confirmed using SDS-PAGE, and this was done after each purification using the fractions collected- flow through, wash 1, wash 2, wash 3, elution, strip, and dialysis.  Figure 4 shows the purification performed in Tris using the Tris purification protocol.  While there is a small amount of protein present in several fractions, the majority of the protein is located in the desired fraction, which was the elution fraction.  The figure also shows that the protein sample is pure, and this is able to be determined by the absence of other bands in the elution and dialyzed sample lanes and the presence of bands around 11 kDa.



Figure 4: SDS-PAGE gel show results for the Ni column affinity purification.

Column 1- Elution fraction
Column 2- Wash 3
Column 3- Wash 2
Column 4- Wash 1
Column 5- Flow through
Column 6- Marker

Once the purity of the protein was confirmed, the concentration of the protein was calculated using UV spectroscopy, and the spectrum obtained is shown in figure 5.
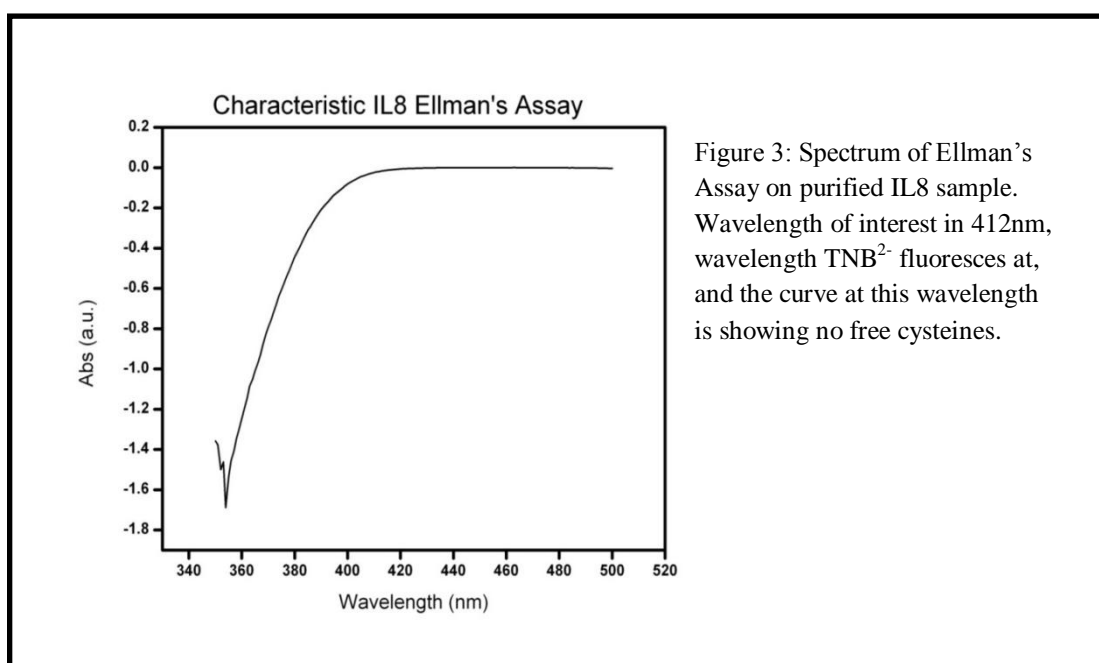


Figure 5: UV spectroscopy spectrum showing absorption of protein sample used to determine the concentration of the protein.
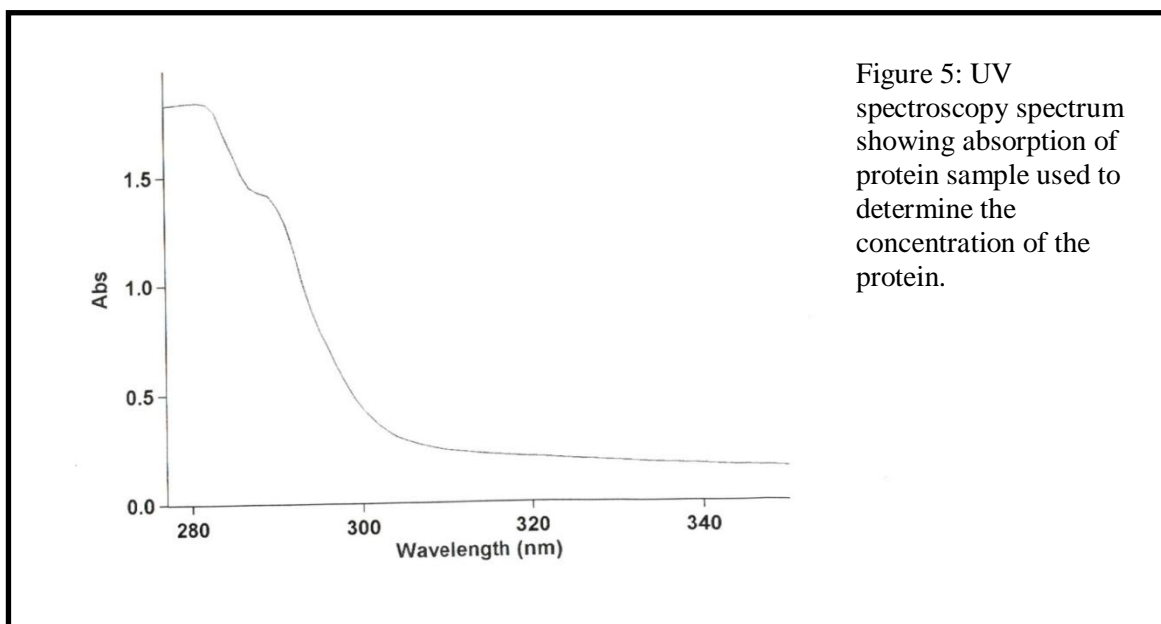
The concentration was calculated to be 26.89 µM, and while this concentration could be used to run minimal experiments, a higher concentration was desired.  To increase the concentration, the protein was concentrated using an Amicon® centrigugal concentrators (Millipore Inc) with a molecular weight cutoff at 3.5 kDa.  A membrane with this molecular weight limit was used because the next size was 10 kDa, and this molecular weight is too close to the molecular weight of interleukin-8 and some of the protein could have been lost in the process.  After concentration, the calculation was determined to be 100 µM.

*IL8 Characterization*

Interleukin-8 contains four cysteines that are paired with one another- Cys-7 binds Cys-4 and Cys-9 binds Cys-50.  The Ellman's Assay was used to determine if all four of

these cysteines were bound and that there were no free cysteines in the protein. When there are free cysteines in a compound, the $TNB^{2-}$ binds to the cysteine and this causes fluorescence; when there are no free cysteines, there isn't anything for the $TNB^{2-}$ to bind to and there isn't anything to fluoresce. Because all of the cysteines are bound in IL8, it was expected that there would not be any fluorescence and the absorbance would be zero at 412 nm, the wavelength $TNB^{2-}$ absorbs at. The spectrum, figure 6, showed that there was no absorbance at 412 nm, confirming that all four of the cysteines in the protein were bound.



Figure 3: Spectrum of Ellman's Assay on purified IL8 sample. Wavelength of interest in 412nm, wavelength $TNB^{2-}$ fluoresces at, and the curve at this wavelength is showing no free cysteines.

Circular dichroism was performed on the sample in order to examine the secondary structure of the protein. The predicted secondary structure of the protein included two alpha helices and six beta sheets, but the CD spectrum, shown in figure 7, did not show the defined peaks and valleys that were expected to correspond with the alpha helices and beta sheets in the IL8 control. Certain minima correspond with particular structures- 208 nm and 222 nm are alpha helices and 216 nm is a beta sheet.

Figure 7: CD of IL-8 control with minima at 224nm and 205nm.
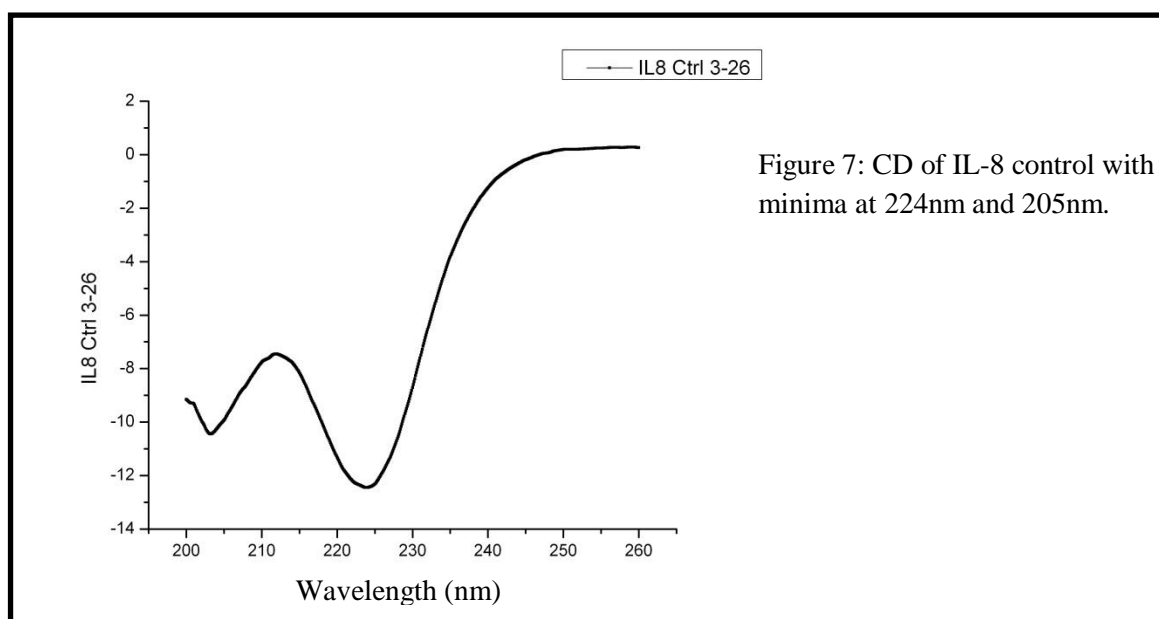
The observed minima in this CD spectrum are 224 nm and 205 nm, which are very close to the predicted minima for the two alpha helices present in the IL8 secondary structure; however, because there are two secondary structures in the protein, one, the alpha helix, shows up more predominantly than the other.

*Mass Spectrometry*

The largest peak on the spectrum, shown in figure 8, is the molecular ion peak and shows the highest mass present in the sample, and the largest peak on this graph is at 11.484 kDa. This value corresponds with the molecular weight of the uncleaved IL8 protein, which has a molecular weight 11.5 kDa.

Figure 8: Spectrum for mass spectrometry confirming purity of IL8.
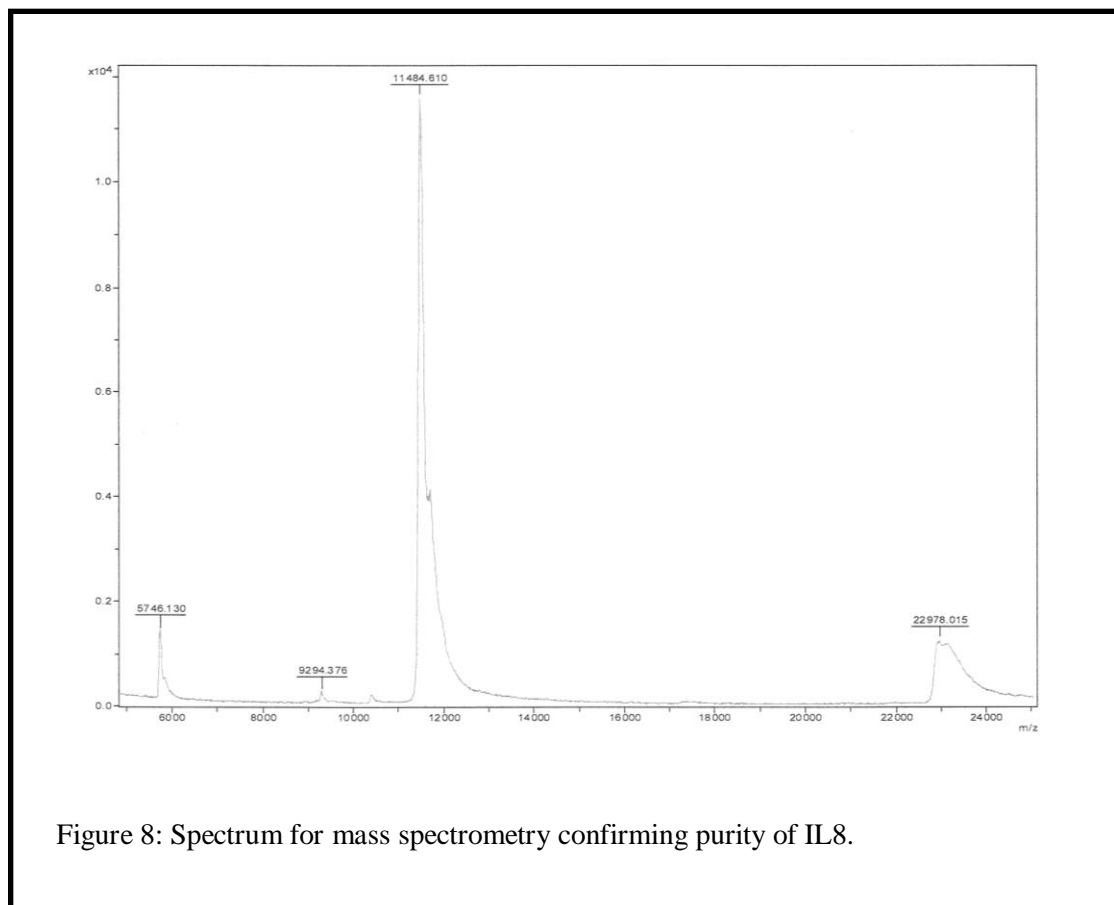
*IL8 and Aβ Interactions*

ThioflavinT fluorescence was used to examine the interactions between Aβ and IL8 over time by measuring the changes in fluorescence that occurred because of fibrilization. Aβ and IL8 controls were used to monitor the aggregation that occurred in the individual samples in order to compare these aggregation levels to the aggregation levels measured in the Aβ and IL8 samples. The IL8 controls increased in concentration from 12.5 uM to 25 uM to 50 uM, and this same increase in sample concentration was used in the Aβ and IL8 samples. The 12.5 uM IL8/Aβ sample was 0.5:1, the 25 uM

IL8/Aβ sample was 1:1, and the 50 uM IL8/Aβ sample was 2:1. The changes in fluorescence were measured for all of the samples over 160 hours and the aggregation levels were compared, and the results are shown in figure 9.



Figure 9: Aβ and IL8 aggregation over 160hours. The spectrum shows the Aβ and IL8 controls, as well as the
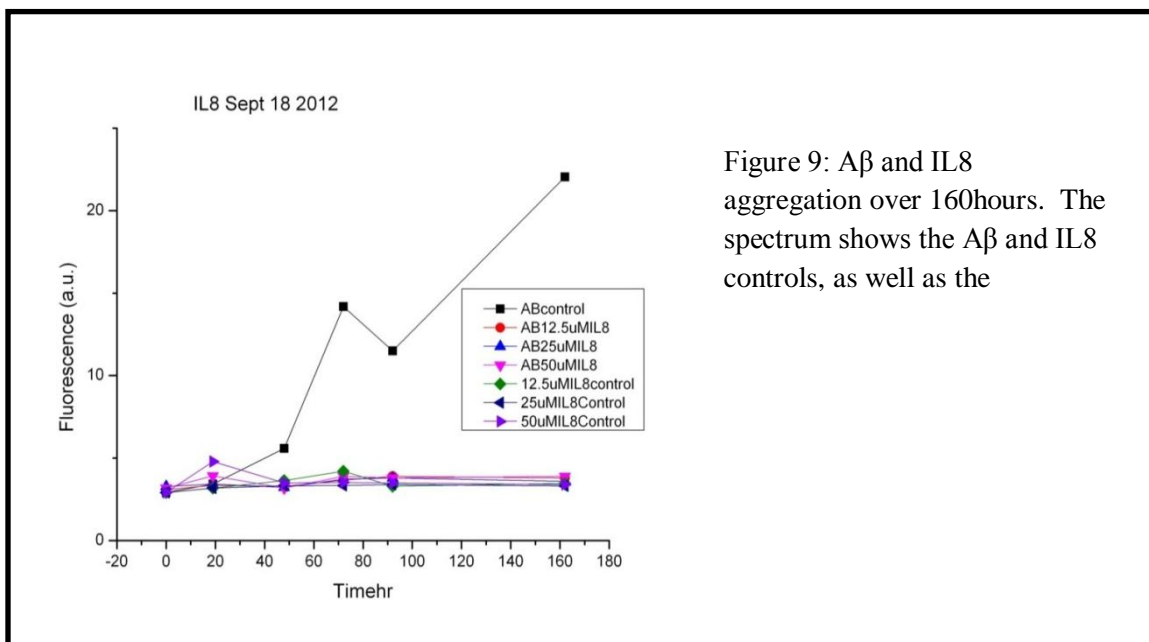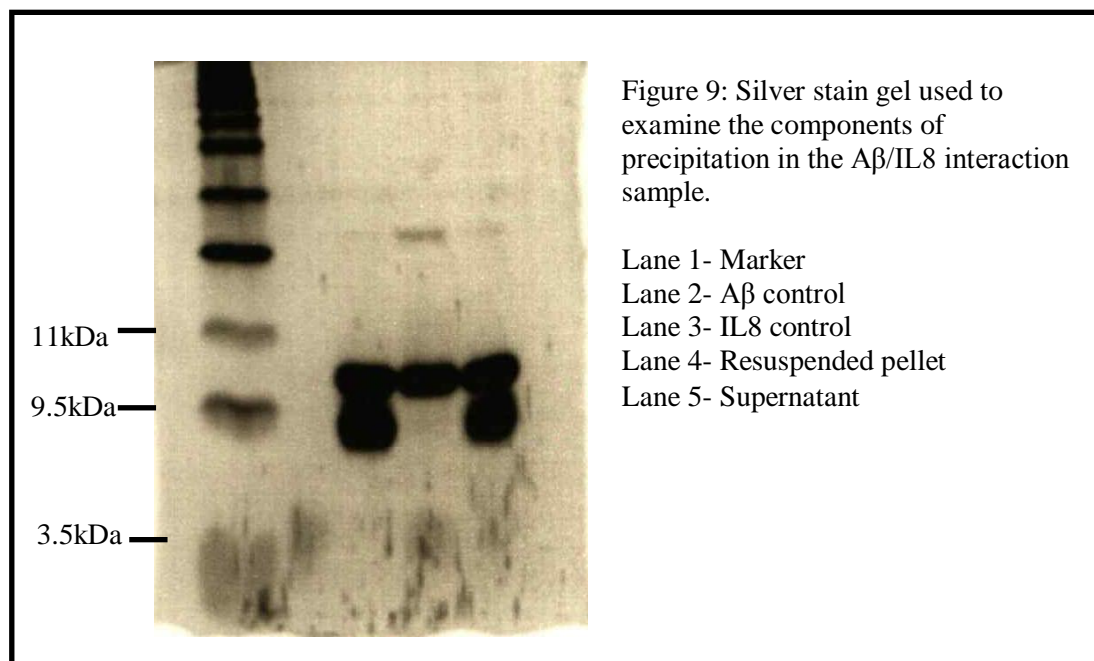
The fluorescence values increase as the level of aggregation increase, so higher A.U. values correspond to more aggregation. This occurs because the ThT binds to the amyloid protein and immobilizes one of the bonds, resulting in fluorescence. As the number of amyloid proteins in the aggregate increases, the amount of ThT that is bound causes an increase in the fluorescence.

When comparing the aggregation rates of the Aβ control, IL8 controls, and Aβ/IL8 incubations, it is clear that the IL8 controls and the Aβ/IL8 incubations at all three of the concentrations had very similar aggregation rates. Comparing this to the Aβ control, it can be seen that there is inhibition of aggregation occurring in the Aβ/IL8 samples because the fluorescence levels in these samples are much lower than the

fluorescence levels of the Aβ control.  The changes in concentration do not appear to cause any change in the inhibition level.

Precipitation was seen in the Aβ/IL8 interaction samples, but not in the Aβ control or IL8 control.  Because the precipitation was only present in the interaction sample, a gel was run in order to determine if the precipitation was caused by an interaction between the two proteins.  The sample containing the precipitation, Aβ/IL8 interaction, was centrifuged at 9500 rpm for twenty minutes to spin the precipitation into a pellet.  The supernatant was then collected and the pellet was resuspended in 150 μL of dialysis buffer.  A gel was loaded with two sets of the samples, which were supernatant, resuspended pellet, IL8 control, and Aβ control, and after the SDS-PAGE was complete, the gel was split in half for silver stain and Western blotting.  Figure 9 shows the results of the silver stain gel.



Figure 9: Silver stain gel used to examine the components of precipitation in the Aβ/IL8 interaction sample.

Lane 1- Marker
Lane 2- Aβ control
Lane 3- IL8 control
Lane 4- Resuspended pellet
Lane 5- Supernatant

The silver stain gel shows only Aβ monomer in the Aβ control found in lane 2, and lane 3 only shows IL8 in the IL8 control. The resuspended pellet sample in lane 4, however, shows only one of the two interleukin-8 bands, the Aβ monomer band, and another band much higher on the gel around 20 kDa. Lane 5 has the two interleukin-8 bands and the Aβ monomer band. The band that appears at 20 kDa in the resuspended pellet sample is mostly likely an IL8 dimer.

# Discussion

*Purification*

In order for the interaction studies to provide useful data, the IL8 used in the aggregation reactions had to be pure so that the interactions between Aβ and IL8 could be examined without the data being confounded by other proteins or cellular debris in the sample. The purity of the IL8 was examined using SDS-PAGE, and the location of a singular band at 11.5 kDa in the elution sample confirmed that the sample contained only the desired IL8. The molecular weight of IL8 is 11.5 kDa, so the presence of the band equal with the 11.5 kDa marker band and lack of any other bands in the sample made it possible to conclude that the protein was purified.

The results present in this research project were achieved using IL8 that was purified using the 20 mM Tris pH 7.0 buffer and the modified 20 mM Tris pH 7.0 buffer, but the Tris protocol was not the only buffer protocol tested for protein purification. Because of precipitation issue, the buffer for the purification was changed from Tris to 20 mM phosphate buffered saline (PBS) pH 6.5 based on a study conducted by Furuta et al (23). When the Tris was used in the purification, there was so much precipitation that the quantity and concentration of the purified protein was unusable. Research was done on different purification protocols for IL8 and a protocol was found to have used 20mM PBS pH 6.5 as the buffer. After switching the purification buffer to PBS, the precipitation issues in the purification were solved and the resulting protein was obtained in higher quantity and concentration; however, precipitation was still an issue in the IL8/Aβ samples used for the ThT experiment. A final change was made to the purification

protocol and the buffer was changed back to 20 mM Tris pH 7.0, but the concentrations of urea were altered. Instead of one wash with 2 M urea, three washes using 6 M, 4 M, and 2 M, respectively, were used, and this was done so the protein could refold at a slower rate and prevent the precipitation. The protein had to be refolded due to the incubation at 8M urea that was done to remove the protein from the inclusion bodies. In each of the column washes, the urea concentration was decreased, but the imidazole concentration was increased, and this was done to compete with the bound His-tag. Imidazole concentrations were constantly increased to elute to protein from the nickel affinity column. When the gel is examined for the purification using the modified Tris protocol, protein can be seen in fractions other than the elution fraction. This loss of protein slightly decreases the quantity and concentration of the protein in the elution sample, but the amount lost is negligible. While this PBS protocol was based on a purification method used by Furuta et al, the concentrations obtained in this study were lower than those outlined in the study, and the precipitation issues were not encountered in the previous study.

*Characterization of IL8*

Ellman's Assay was done to quantify the free cysteines in IL8, and the results of this assay confirmed that there were not any free cysteines in the pure protein. This assay does not, however, show if the cysteines are bound to the correct cysteine. Cys-7 binds to Cys-4 and Cys-9 binds to Cys-50 in a correctly folded protein. Based on the results of this characterization experiment, we can conclude that there are the proper number of disulfide bonds in the purified protein, but not that the correct pairing has occurred.

Circular Dichroism was used to examine the secondary structure of IL8 to make sure the protein was in the proper conformation. When the spectrum is examined, the two minima for the alpha helices were observed.

*Aβ and IL-8 Interactions*

ThT fluorescence was used to monitor aggregation in the samples over time. The spectrum presented previously was obtained using IL8 that was purified using the modified Tris protocol, and the results show clear inhibition of Aβ aggregation in the Aβ/IL8 samples. The Aβ control curve closely follows, with the exception of the 68hr point, the sigmoidal growth curve of Aβ. This curve consists of a lag phase, seen from zero to fifty hours, a growth phase, seen from 50 to 160 hours, and the eventual stationary phase, which had not yet been reached when this experiment was halted. The concentration of the IL8 in the Aβ/IL8 interactions does not appear to make a significant difference in inhibition, as demonstrated by the spectrum. This lack of concentration dependence is significant because it shows that lower levels of IL8 in the brain have the same effect as high protein concentrations, and this could be used to a therapeutic advantage.

When similar aggregation studies were conducted using PBS as the purification buffer, the inhibitory results seen in the initial Tris experiments were not replicated. Instead, there was so much precipitation that accurate fluorescence reading could not be obtained. Yet another set of aggregation studies was tried using the modified Tris protocol, and while the results were similar to the initial Tris aggregation results, precipitation was still an issue. Visible precipitation was seen in the Aβ/IL8 interaction

sample within one hour of sample preparation. The aggregation in this sample was examined using SDS-PAGE to determine the components of the precipitate.

When the silver stain gel containing the samples of the supernatant and resuspended pellet from the precipitated Aβ/IL8 sample is examined, the resuspended pellet sample shows an Aβ monomer band, a single IL8 band, and an additional band at 20 kDa. The supernatant sample only contains the expected two IL8 bands and the Aβ monomer band. Based on the molecular weight of the 20 kDa band, it is believed that this band is an IL8 dimer.

Along with ThT fluorescence, SDS-PAGE has been used to examine the aggregation in the interaction samples. Using these gels, it has been found that IL-8 could possible undergo a conformational change after 48hours of incubation, and this is conclusion was reached based on the presence of two bands, one at approximately 11kDa and the other at 9kDa, after 48hours in the IL8 control sample. These two bands have been seen in every sample containing IL8 after the 48hour mark.

Future work for this project includes performing the cleavage on IL8 to remove the His-tag and examining the changes that occur in the protein, exploring the conformational change that is indicated by the change in molecular weight, and examine the precipitation issues caused by difference in buffer in pH.

Overall, the research suggests that IL8 plays an inhibitory role in the aggregation of Aβ. The purification protocol using Tris buffer has been standardized, and once a solution for the precipitation in the Aβ/IL8 samples has been found, additional studies can be performed examining this inhibition.

**Literature Cited**

1. Selkoe, Dennis J. (2001) Alzheimer's Disease: Genes, Proteins, and Therapy. *Physiol Reviews 81*(2), 741-766

2. Haass, C., and Selkoe, D.J. (2007) Soluble protein oligomers in neurodegeneration: lessons from the Alzheimer's amyloid beta-peptide, *Nat Rev Mol Cell Biol 8*, 101-112

3. Harada et al. (1994) Essential involvement of interleukin-8 (IL-8) in acute inflammation. *Journal of Leukocyte Biology 56*, 559-564

4. Ahmed et al. (2007) Progranulin in frontotemporal lobar degeneration and neuroinflammation. *Journal of Neuroinflammation 4(7)*, 1-13

5. Gopcevic et al. (2007) Plasma Interleukin-8 as a Potential Predictor of Mortality in Adult Patients with Severe Traumatic Brain Injury. *Tohoku Journal of Experimental Medicine 211,* 387-393

6. Pereson et al. (2009) Progranulin expression correlates with dense-core amyloid plaque burden in Alzheimer disease mouse models. *Journal of Pathology 219*, 173-181

7. Tolkatchev et al. (2008) Structure dissection of human progranulin identifies well-folded granulin/epithelin modules with unique functional activities. *Protein Science 17,* 711-724

8. He et al. (2003) Progranulin is a mediator of the wound response. *Nature Medicine 9*, 225-229

9. Kuman-Singh, S. (2007) Cerebral amyloid angiopathy: pathogenetic mechanisms and link to dense amyloid plaques. *Genes, Brain and Behavior 7*, 67-82

10. Walsh et al. (1997) Amyloid beta- protein fibrillogenesis. Detection of a protofibrillar intermediate. *Journal of Biological Chemistry 272,* 22364-22372

11. Rogers, Joseph. (2008) The Inflammatory Response in Alzheimer's Disease. *Journal of Periodontology 10*, 1535-1543

12. Vendramini et al. (2011) Interleukin-8-251T> A, Interleukin-1α-889C > and Apolipoprotein E polymorphisms in Alzheimer's Disease. *Genetics and Molecular Biology 34 (1),* 1-5

13. Friedrich et al. (2010) Mechanism of amyloid plaque formation suggests an intracellular basis of Aβ pathogenicity. *PNAS 107 (5)*, 1942-1947

14. Grammas, Paul. (2011) Neurovascular dysfunction, inflammation and endothelial activation: Implications for the pathogenesis of Alzheimer's Disease. *Journal of Neuroinflammation 26 (8),* 1-12

15. Ghirnikar et al. (1998) Inflammation in Traumatic Brain Injury: Role of Cytokines and Chemokines. *Neurochemical Research 23 (3),* 329-340

16. Bateman, A. , Bennett, H. P. J. (1998) Granulins: the structure and function of an emerging family of growth factors. *Journal of Endocrinology 158,* 145-151

17. Lue et al. (1999) Soluble Amyloid β Peptide Concentration as a Predictor of Synaptic Change in Alzheimer's Disease. *American Journal of Pathology 155 (3),* 853- 862

18. Bateman, A., Bennett, H. P. J. (2009) The granulin gene family: from cancer to dementia. *BioEssays 31,* 1245-1254

19. Kindt et al. (2007) Immunology. W. H. Freeman and Company. New York, NY.

20. Neher et al. (2011) Molecular meachanisms of inflammation and tissue injury after major trauma-is complement the "bad guy"?. *Journal of Biomedical Science, 18:90*.

21. Centers for Disease Control and Prevention. Injury Prevention and Control: Traumatic Brain Injury. http://www.cdc.gov/traumaticbraininjury/. March 18, 2013. Date accessed March 28, 2013.

22. Ziebell, J. M., Morganti-Kossmmann, M. C. Involvement of Pro- and Anti-Inflammatory Cytokines and Chemokines in the Pathophysiology of Traumatic Brain Injury. *Neurotherapeutics: The Journal of the American Society for Experimental Neurotherapeutics. 7*, 22-30.

23. Furuta et al. (1989) Production and Characterization of Recombinant Human Neutrophil Chemotactic Factor. *Journal of Biochemistry. 106*, 436-441.